

Squeezing a Surface Plasmon through Quadratic Nonlinear Interactions

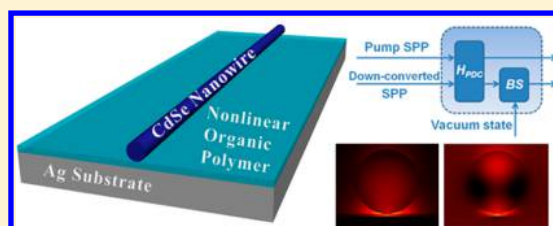
Yang Ming, Weihua Zhang, Zhaoxian Chen, Zijian Wu, Jie Tang, Fei Xu, Lijian Zhang,* and Yanqing Lu*

National Laboratory of Solid State Microstructures, College of Engineering and Applied Sciences, Collaborative Innovation Centre of Advanced Microstructures, Nanjing University, Nanjing 210093, China

Supporting Information

ABSTRACT: Quantum plasmonics presents a new insight into quantum photonic science and technology. The unique properties of surface plasmon polaritons (SPPs) provide immense potential for quantum control of light in ultracompact systems. The quantum behavior of SPPs should be described by corresponding SPP states, which have attracted a lot of investigative interest recently. In this work, we focus on the interaction of single quanta of SPPs. The generation of a squeezed SPP state through parametric down conversion (PDC) is investigated. Due to intrinsic loss of an SPP, this system deviates from those based on traditional bulk optics. Unlike the previous negative image, it is surprising to find that the role of loss is partly positive. As an illustration, the squeezing process of an SPP in a hybrid plasmonic waveguide system is calculated and shown. The degree of squeezing could reach above 7 dB with a propagation length of only about 12 μm in a single path. Moreover, the spectrum of squeezing has a band of 481.7 THz. It is a valuable advantage to keep a high squeezing degree in such a wide band, which is hard to realize in bulk systems. In addition, the tolerance of the system to loss is also shown to be good. The plasmonic system exhibits an attractive advantage in constructing integrated quantum circuits.

KEYWORDS: quantum plasmonics, squeezed surface plasmon state, intrinsic loss



A surface plasmon polariton (SPP) is an electromagnetic surface wave propagating at the metal–dielectric interface, which originates from the interaction between electromagnetic fields and electron plasma in a metal.¹ Owing to the unique property of subwavelength field confinement, an SPP has exhibited a great value in nanophotonics.^{2,3} Adequate quantities of plasmonic devices are proposed and demonstrated at the level of classical optics,^{4–12} which show excellent performances. For a step further, researchers take a lively interest in discovering the potential of SPPs for the quantum control of light.^{13,14} Several intriguing investigations on the quantum properties of SPPs are reported, including plasmon-assisted entanglement survival,^{15–18} the quasi-particle nature of SPPs,^{13,14,17,19–22} wave–particle duality,²³ the quantum statistics properties of SPPs,^{21,22} and two-plasmon quantum inference.^{24,25} In addition, many other unknown quantum properties need to be further explored for a systemic and detailed quantum description of SPPs.

The nonclassical states are always important resources for quantum information processing. Among them, the squeezed state is a most useful one that has crucial applications in quantum metrology^{26,27} and continuous-variable quantum communication.²⁸ It is demonstrated that optical nanostructures can be utilized for controlling the squeezed light,²⁹ and the plasmon–polariton resonance plays an important role. Combining the squeezed state with an SPP may allow us to achieve unprecedented precision in sensing as well as manipulating the interactions of quantum light and matter at

the subwavelength scale. Previous works have verified that SPPs could preserve nonclassical properties through launching squeezed light into a plasmonic waveguide and detecting the squeezing degree of the output light.^{30–32} However, little attention has been paid to the essence of SPP squeezing, namely, the rearrangement of fluctuations between amplitude and phase quadratures^{33–37} arising from the interaction of a single quanta. In this work, we investigate generating an SPP squeezed state through the nonlinear interaction of single surface plasmons. Due to the local field enhancement and intrinsic loss of SPPs, the situation is quite different from that in traditional bulk optics. Distinguished from the usual impediment of the performances of plasmonic systems, it is surprising to find that the role of loss here is partly positive. Although a squeezing limit is brought into the system, the effective coupling coefficient of the parametric down conversion process is enhanced, which means the squeezing length corresponding to a certain squeezing degree is greatly reduced compared to those in bulk optics. Moreover, a practical plasmonic structure is proposed to show the squeezing results. The squeezing degree of the generated nonclassical SPP state could reach above 7 dB with a propagation length of only 12 μm in a single-pass configuration. The bandwidth of the squeezing spectrum can be as high as 481.7 THz. This is an important advantage over bulk squeezing systems, in which it is hard to obtain a high

Received: June 21, 2016

Published: October 5, 2016

squeezing degree and a wide squeezing band at the same time. In addition, the compact feature of this device is significant in constructing integrated quantum photonic circuits.

RESULTS AND DISCUSSION

Squeezing an SPP through Parametric Down Conversion. The usually used method to investigate the quantum properties of SPPs is to generate a nonclassical photonic state and inject it into plasmonic structures, then examine whether the corresponding quantum properties survive.^{15–19,21–25,30} These results provide important evidence for the quantum nature of SPPs. However, as the nonclassical properties are transferred to SPPs from the incident photons, the SPP actually plays an intermediate role in such systems. It is still necessary to acquire a description of nonclassical SPP states from the level of the interaction of a single SPP quanta. For photons, nonlinear optical interactions devote a convenient platform for generating nonclassical states such as squeezed states^{34–36} or entangled photon states.^{38–41} Inspired by these interactions, we consider squeezing an SPP through parametric down conversion. Recent developments of nonlinear plasmonics also provide relevant bases.^{42–48}

For nonlinear interaction processes of SPPs, the intrinsic loss is a key influence factor.^{43–47} Owing to loss, the electromagnetic energy is not conserved, so we could not obtain a global Hamiltonian for a plasmonic system. To solve this problem, we adopt an equivalent method. It is shown that the transmission of squeezed light through a plasmonic waveguide could be described by a beam splitter relation with an additional vacuum input.³⁰ On the basis of this result, a differential approach could be utilized to study the parametric down conversion of an SPP. The corresponding plasmonic structure may be divided into a large number of differential elements along the propagation direction. In each element, the lossy nonlinear interaction process of SPPs is equivalent to two cascaded subprocesses. For the first subprocess, we attempt to obtain a local Hamiltonian to describe the interaction of SPPs. The corresponding attenuation should be properly dealt with to ensure a locally lossless situation. The pump field is assumed to be classical,⁴⁹ and the influence of its attenuation could be included in the coupling coefficient. The down-converted SPPs are treated as quantized fields. Their attenuation is separated from this subprocess, which would be considered in the next one through an equivalent beam splitter transformation. All the processes are illustrated in Figure 1a and c.

It could be seen from the figures that a dz -element is regarded as a cell (z is the propagation direction). The down-converted SPP state is cascadingly squeezed through the locally lossless Hamiltonian operation and mixed with a vacuum state in each cell. The final output SPP state could be obtained by combining all these cells in sequence.

To clarify the basic physical principles in the squeezing process of the SPP, we first investigate single-mode squeezing in the perfectly phase-matched case; then discussions are extended to more general cases. For our simplified case, the pump field is set to be monochromatic and continuous, and the down-converted frequencies are degenerate. The corresponding expressions are as follows:

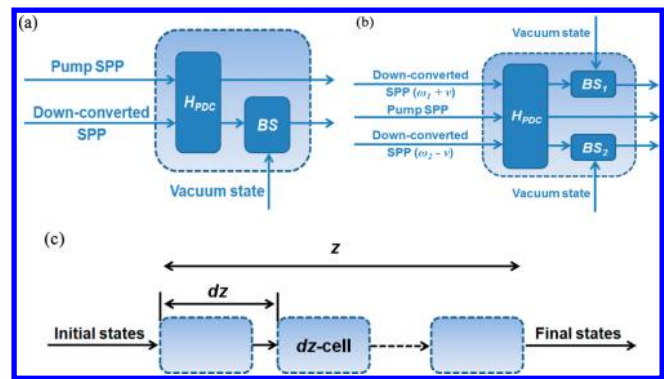


Figure 1. Schematic diagram of the squeezing SPP process. Detailed configuration of a dz -cell for (a) degenerate parametric down conversion and (b) nondegenerate parametric down conversion. The total squeezing process in a dz -element is divided into two subprocesses. The interaction of pump and down-converted SPPs is assumed to be locally lossless, and the influence of the pump loss is included in the local coupling coefficient. The loss of the down-converted SPPs is equivalent to a beam splitter transformation. (c) The final squeezing result could be derived through cascading all dz -cells.

$$E_p(\vec{r}, t) = A_p(z) \Phi_p(x, y) e^{i(\beta_p z - \omega_p t + \varphi_0)} + \text{complex conjugate}$$

$$E_s(\vec{r}, t) = \sqrt{\frac{\hbar \omega_s}{2 \epsilon_0 L_z}} \Phi_s(x, y) a_{\text{SPP}}^\dagger e^{-i(\beta_s z - \omega_s t)} + \text{Hermitian conjugate} \quad (1)$$

In the equations, $\Phi_p(x, y)$ and $\Phi_s(x, y)$ are transverse profiles of corresponding SPP modes,^{19,20,50} while β_p and β_s represent propagation constants. $A_p(z)$ is the amplitude of the pump field. The initial phase of the pump field is set at φ_0 . The creation and annihilation operators are expressed as $\{a_{\text{SPP}}^\dagger, a_{\text{SPP}}\}$. If the phase matching condition is satisfied, we could obtain the interaction Hamiltonian as

$$H_I = \frac{1}{2} \int_V d^3r P_{\text{NL}} E = \frac{\epsilon_0}{2} \int dV \chi^{(2)} E_p(\vec{r}, t) [E_s(\vec{r}, t)]^2$$

$$= \frac{\hbar \chi^{(2)} \omega_s}{4} A_p(z) \left(\iint dx dy \Phi_p \Phi_s^2 \right) [a_{\text{SPP}}^2 e^{i\varphi_0} + (a_{\text{SPP}}^\dagger)^2 e^{-i\varphi_0}] \quad (2)$$

It could be seen from the equation that $A_p(z)$ is an important parameter of the interaction Hamiltonian. The value of $A_p(z)$ is influenced by the intrinsic loss and the power flowing into the down-converted fields. Owing to the extremely low transformation efficiency of the parametric down conversion process, the latter effect is negligible.³³ As $A_p(z)$ varies, the locally lossless Hamiltonians for corresponding dz -cells are different. Yet if the pump SPP gets a 100% compensation, as demonstrated in the recent experiments, Hamiltonians in all dz -cells are the same.⁵¹ Since this is the most efficient configuration to utilize the pump power, we will focus on this situation. The evolution equations for down-converted SPPs in each dz -cell can be obtained as

$$\begin{aligned} \dot{a}_z &= \frac{1}{i\hbar} [a_z, H_{1,z}] = -i\Omega_{1,z} a_z^\dagger e^{-i\varphi_0} \\ \dot{a}_z^\dagger &= \frac{1}{i\hbar} [a_z^\dagger, H_{1,z}] = i\Omega_{1,z} a_z e^{i\varphi_0} \end{aligned} \quad (3)$$

with

$$\Omega_{1,z} = \frac{\chi^{(2)} \omega_s}{2} A_p(z) \left(\iint dx dy \Phi_p \Phi_s^2 \right) \quad (4)$$

From the equations above, it can be seen that the mode overlap is a crucial factor that has great influence on the squeezing of an SPP. The overlap includes two aspects, the integrals of $\Phi_p(x, y)$ and $\Phi_s(x, y)$ and the portion of the integral in the nonlinear medium.

If the initial phase φ_0 is set to be $\pi/2$, the transformation matrix of operators in each dz -cell could be expressed as

$$M_{sq}(z) = \begin{bmatrix} \cosh[(\Omega_{1,z} n_{\text{PDC}}/c) dz] & -\sinh[(\Omega_{1,z} n_{\text{PDC}}/c) dz] \\ -\sinh[(\Omega_{1,z} n_{\text{PDC}}/c) dz] & \cosh[(\Omega_{1,z} n_{\text{PDC}}/c) dz] \end{bmatrix} \quad (5)$$

then we have

$$\begin{bmatrix} a_{z,sq} \\ a_{z,sq}^\dagger \end{bmatrix} = \begin{bmatrix} \cosh[(\Omega_{1,z} n_{\text{PDC}}/c) dz] & -\sinh[(\Omega_{1,z} n_{\text{PDC}}/c) dz] \\ -\sinh[(\Omega_{1,z} n_{\text{PDC}}/c) dz] & \cosh[(\Omega_{1,z} n_{\text{PDC}}/c) dz] \end{bmatrix} \begin{bmatrix} a_{z,in} \\ a_{z,in}^\dagger \end{bmatrix} \quad (6)$$

After the Hamiltonian operation, the attenuation in the corresponding dz -cell could be considered through a beam splitter transformation with an additional vacuum input, which is expressed as^{52–54}

$$\begin{bmatrix} a_{z,out} \\ a_{z,out}^\dagger \end{bmatrix} = \sqrt{T_{dz}} \begin{bmatrix} a_{z,sq} \\ a_{z,sq}^\dagger \end{bmatrix} + \sqrt{R_{dz}} \begin{bmatrix} a_{z,v} \\ a_{z,v}^\dagger \end{bmatrix} \quad (7)$$

In the equations, $\{a_{z,v}, a_{z,v}^\dagger\}$ corresponds to the vacuum state. In fact, another method to deal with the problems with the absorption losses is based on the master equation with Liouvillian terms.³³ Nevertheless, it has been proved that the dissipation process described by the Liouvillian formulation is equivalent to mixing the input field with a single fluctuation mode (the vacuum mode in our case) at a beam splitter, even when the reservoir for the dissipation carries many degrees of freedom.⁵⁵ Details of the proof can be found in the [Supporting Information](#).

Through these two procedures, the output state of a dz -cell is related to its input. The final squeezed SPP state could be calculated via combining the transformations of all dz -cells, and the recurrence formula is expressed as

$$\begin{bmatrix} a_{z_{n+1},in} \\ a_{z_{n+1},in}^\dagger \end{bmatrix} = \sqrt{T_{dz}} \times \begin{bmatrix} \cosh[(\Omega_{1,z} n_{\text{PDC}}/c) dz] & -\sinh[(\Omega_{1,z} n_{\text{PDC}}/c) dz] \\ -\sinh[(\Omega_{1,z} n_{\text{PDC}}/c) dz] & \cosh[(\Omega_{1,z} n_{\text{PDC}}/c) dz] \end{bmatrix} \times \begin{bmatrix} a_{z_n,in} \\ a_{z_n,in}^\dagger \end{bmatrix} + \sqrt{R_{dz}} \begin{bmatrix} a_{z_n,v} \\ a_{z_n,v}^\dagger \end{bmatrix} \quad (8)$$

In the case of 100% pump compensation, the calculations could be simplified, and an analytic expression of the final state is achievable. The corresponding formula is as follows (more details about the derivation process can be found in the [Methods](#) section):

$$\begin{aligned} a_{\text{final},g} &= \sqrt{T_{\text{tot}}} [\cosh(\Omega_{1,g} n_{\text{PDC}} L_0/c) a_{\text{in}} - \sinh(\Omega_{1,g} n_{\text{PDC}} L_0/c) a_{\text{in}}^\dagger] \\ &\quad + \sum_{\{z_n\}} \sqrt{R_{dz}} \sqrt{T_{\text{tot}}/T_{z_n}} \{ \cosh[\Omega_{1,g} n_{\text{PDC}}(L_0 - z_n)/c] a_{z_n,v} \\ &\quad - \sinh[\Omega_{1,g} n_{\text{PDC}}(L_0 - z_n)/c] a_{z_n,v}^\dagger \} \\ a_{\text{final},g}^\dagger &= \sqrt{T_{\text{tot}}} [\cosh(\Omega_{1,g} n_{\text{PDC}} L_0/c) a_{\text{in}}^\dagger - \sinh(\Omega_{1,g} n_{\text{PDC}} L_0/c) a_{\text{in}}] \\ &\quad + \sum_{\{z_n\}} \sqrt{R_{dz}} \sqrt{T_{\text{tot}}/T_{z_n}} \{ \cosh[\Omega_{1,g} n_{\text{PDC}}(L_0 - z_n)/c] a_{z_n,v}^\dagger \\ &\quad - \sinh[\Omega_{1,g} n_{\text{PDC}}(L_0 - z_n)/c] a_{z_n,v} \} \end{aligned} \quad (9)$$

In the equations, T_{tot} represents the total transmission efficiency of L_0 , while T_{z_n} corresponds to the transmission efficiency of a length z_n . R_{dz} is the reflection efficiency of the equivalent beam splitter in a dz -cell, and $\Omega_{1,g}$ are shown in eq 4 and are the same in all dz -cells. From eq 9, the physical meaning of the squeezing process of an SPP could be clearly seen. At each z -position, a vacuum state is injected into the system and goes on to be squeezed in the remaining interaction region until the output port (in fact, the initial input state at $z = 0$ is also a vacuum state). The final squeezing results are determined by the superposition of all these subprocesses. Through the creation and annihilation operators of the final squeezed state, the two corresponding quadratures could be expressed as

$$\begin{aligned} X_1 &= (a_{\text{final},g} + a_{\text{final},g}^\dagger)/2 \\ X_2 &= (a_{\text{final},g} - a_{\text{final},g}^\dagger)/2i \end{aligned} \quad (10)$$

Thus their fluctuations are obtained as

$$\begin{aligned} \langle \Delta X_1 \rangle^2 &= \frac{T_{\text{tot}}}{4} [\cosh(\Omega_{1,g} n_{\text{PDC}} L_0/c) - \sinh(\Omega_{1,g} n_{\text{PDC}} L_0/c)]^2 \\ &\quad + \frac{1}{4} \sum_{\{z_n\}} (R_{dz} T_{\text{tot}}/T_{z_n}) \\ &\quad \times \{ \cosh[\Omega_{1,g} n_{\text{PDC}}(L_0 - z_n)/c] - \sinh[\Omega_{1,g} n_{\text{PDC}}(L_0 - z_n)/c] \}^2 \\ \langle \Delta X_2 \rangle^2 &= \frac{T_{\text{tot}}}{4} [\cosh(\Omega_{1,g} n_{\text{PDC}} L_0/c) + \sinh(\Omega_{1,g} n_{\text{PDC}} L_0/c)]^2 \\ &\quad + \frac{1}{4} \sum_{\{z_n\}} (R_{dz} T_{\text{tot}}/T_{z_n}) \\ &\quad \times \{ \cosh[\Omega_{1,g} n_{\text{PDC}}(L_0 - z_n)/c] + \sinh[\Omega_{1,g} n_{\text{PDC}}(L_0 - z_n)/c] \}^2 \end{aligned} \quad (11)$$

In the equations, we have $T_{\text{tot}} = e^{-\alpha_{\text{PDC}} L_0}$ and $T_{z_n} = e^{-\alpha_{\text{PDC}} z_n}$, where the parameter α_{PDC} represents the attenuation coefficient

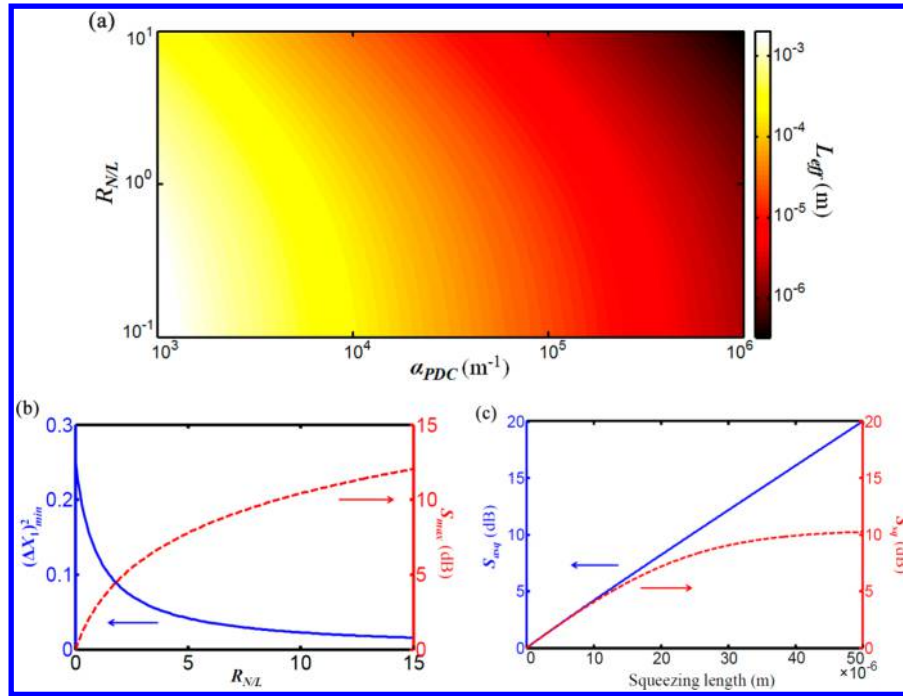


Figure 2. Squeezing of SPP in the degenerate parametric down conversion case. (a) Values of effective squeezing length with different ratios of nonlinear gain to loss ($R_{N/L} = 2\Omega_{lg}n_{PDC}/\alpha_{PDC}$) and loss of down-converted SPP (α_{PDC}). (b) Values of minimum quadrature fluctuation $(\Delta X_1)^2$ and maximum squeezing degree vary with the ratio of nonlinear gain to loss ($R_{N/L}$). (c) Degrees of squeezing and antisqueezing vary with squeezing length for the case in which $R_{N/L} = 10$ and $\alpha_{PDC} = 1 \times 10^4$ m $^{-1}$.

of the down-converted SPP. As $R_{dz} = 1 - T_{dz} = 1 - e^{-\alpha_{PDC}dz} \approx \alpha_{PDC} dz$, the expressions could be transformed into integrals as

$$\begin{aligned} \langle \Delta X_1 \rangle^2 &= \frac{1}{4} T_{tot} e^{-\Omega_{lg}n_{PDC}L_0/c} (1 + \alpha_{PDC} \int_0^{L_0} dz e^{\alpha_{PDC}z} e^{2\Omega_{lg}n_{PDC}z/c}) \\ &= \frac{1}{4} \frac{2\Omega_{lg}n_{PDC}/c}{\alpha_{PDC} + 2\Omega_{lg}n_{PDC}/c} e^{-(\alpha_{PDC} + 2\Omega_{lg}n_{PDC}/c)L_0} \\ &\quad + \frac{1}{4} \frac{\alpha_{PDC}}{\alpha_{PDC} + 2\Omega_{lg}n_{PDC}/c} \end{aligned} \quad (12)$$

Similarly, we have

$$\begin{aligned} \langle \Delta X_2 \rangle^2 &= \frac{1}{4} \frac{2\Omega_{lg}n_{PDC}/c}{2\Omega_{lg}n_{PDC}/c - \alpha_{PDC}} e^{(2\Omega_{lg}n_{PDC}/c - \alpha_{PDC})L_0} \\ &\quad + \frac{1}{4} \frac{\alpha_{PDC}}{\alpha_{PDC} - 2\Omega_{lg}n_{PDC}/c} \end{aligned} \quad (13)$$

Analyzing eqs 12 and 13, it is found that there are two main influences of intrinsic attenuation on the squeezing process of an SPP. First, attenuation drives the system to deviate from the ideal case in a lossless quadratic nonlinear optical medium and brings a squeezing limit. That means the squeezing becomes saturated at large propagation length. An effective squeezing length thus can be defined. Considering both the degrees of squeezing and antisqueezing, it is set at the length corresponding to 90% of the maximal squeezing degree. The reference values are shown in Figure 2a. It is seen that the effective length is no longer than millimeter-scale. In such a situation, for a usually used pump laser with a power of 10^{-1} – 10^1 W, the total loss should be no larger than 100; thus the pump power is far from the quanta level. Moreover, the

negative influence of attenuation on squeezing the SPP can be restrained through increasing the nonlinear optical gain, which is defined as $2\Omega_{lg}n_{PDC}/c$. The limit degree of squeezing increases with the ratio of nonlinear optical gain to loss ($R_{N/L} = 2\Omega_{lg}n_{PDC}/\alpha_{PDC}$), as is shown in Figure 2b. When the ratio reaches about 10, the squeezing limit could be larger than 10 dB, which is a high value even for the setup with optical cavities.⁵⁶ As a result, the practical applications of squeezing an SPP are not seriously affected by the attenuation. Second, due to the competition between squeezing and losses,⁵⁷ the effective coupling coefficient of the parametric down conversion process becomes larger (the attenuation coefficient α_{PDC} is added to the nonlinear gain in the power of an exponential function). As an advantage, the squeezing length corresponding to a certain squeezing degree is shortened. That is a valuable characteristic for integrated quantum circuits, which means the corresponding devices could be more compact. In addition, instead of obtaining a higher squeezing degree, increasing the device length brings a greater antisqueezing noise. A detailed case is calculated with a ratio 10 and $\alpha_{PDC} = 1 \times 10^4$ m $^{-1}$, as shown in Figure 2c.

When the pump compensation is below 100%, the calculations become complex and analytic expressions are unavailable, but the squeezing process could still be derived based on the differential approach discussed above. The squeezing result of a given system is obtainable through numerical calculations. For general cases in which the down-converted frequencies are nondegenerate and the natural bandwidth of parametric down conversion is considered, the differential approach is also feasible, but the dz -cell should be reconfigured. Both the operators of signal and idler SPPs should be considered in the evolution equations, and the influence of phase matching ought to be included. The equations are expressed as^{33,56}

$$\frac{da_{\omega_1+\nu,z}}{dz} = i\Omega_{\text{I,nd}}(\omega_1 + \nu, \omega_2 - \nu; z)a_{\omega_2-\nu,z}^\dagger e^{i\Delta\beta z}$$

$$\frac{da_{\omega_2-\nu,z}^\dagger}{dz} = -i\Omega_{\text{I,nd}}^*(\omega_1 + \nu, \omega_2 - \nu; z)a_{\omega_1+\nu,z} e^{-i\Delta\beta z}$$
(14)

with

$$\Omega_{\text{I,nd}}(\omega_1 + \nu, \omega_2 - \nu; z) = \frac{\chi^{(2)}\sqrt{(\omega_1 + \nu)(\omega_2 - \nu)}}{2} A_p(z)$$

$$\times \left[\iint dx dy \Phi_p \Phi_s(\omega_1 + \nu) \Phi_i(\omega_2 - \nu) \right]$$
(15)

In the equations, we have $\Delta\beta = \beta_p - \beta_s(\omega_1 + \nu) - \beta_i(\omega_2 - \nu)$, where the signal and idler frequencies are defined as $\omega_1 + \nu$ and $\omega_2 - \nu$. Then, the down-converted signal and idler states are mixed with corresponding vacuum states as

$$a_{\omega_1+\nu,z,\text{out}} = \sqrt{T_{\omega_1+\nu,dz}} a_{\omega_1+\nu,z,\text{sq}} + \sqrt{R_{\omega_1+\nu,dz}} a_{\omega_1+\nu,z,v}$$

$$a_{\omega_2-\nu,z,\text{out}} = \sqrt{T_{\omega_2-\nu,dz}} a_{\omega_2-\nu,z,\text{sq}} + \sqrt{R_{\omega_2-\nu,dz}} a_{\omega_2-\nu,z,v}$$
(16)

where $a_{\omega_1+\nu,z,v}$ and $a_{\omega_2-\nu,z,v}$ are corresponding vacuum operators. $R_{\omega,dz}$ is the reflectivity that is equal to $1 - e^{-\alpha_{\text{PDC}}(\omega)dz} \approx \alpha_{\text{PDC}}(\omega)dz$, and $T_{\omega,dz}$ is equal to $1 - R_{\omega,dz}$. This process is shown in Figure 1b. The final squeezing result could be derived through cascading all dz -cells together.

Generation of Squeezed SPP State in a Hybrid Plasmonic Waveguide System. For a distinct view of the squeezed SPP state, we investigate the squeezing process of an SPP in a typical hybrid plasmonic waveguide,^{7,58,59} as shown in Figure 3a. This structure is selected according to the following considerations. First, the eigen-SPP mode of this structure is of a high degree of two-dimensional confinement. Correspondingly, the overlap between the pump and the down-converted modes is extremely large. Second, the intrinsic loss of the SPP mode in the present configuration is quite low. Third, as the

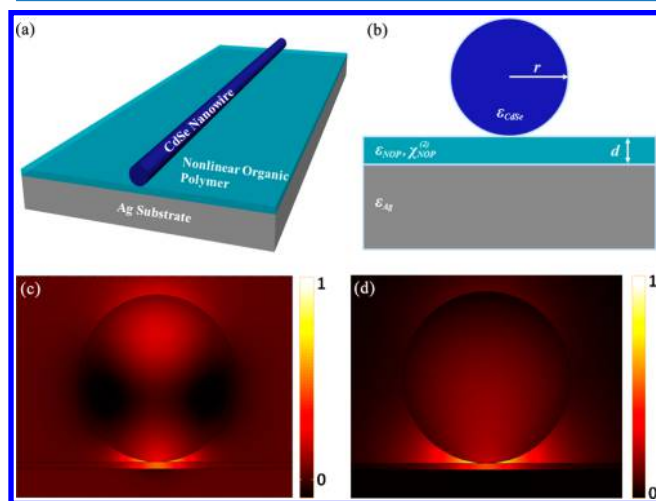


Figure 3. Hybrid plasmonic waveguide system. (a) Schematic of the waveguide structure. (b) Transverse geometry. The pump and down-converted SPP modes with wavelengths of (c) 775 nm and (d) 1550 nm when $d = 20$ nm and $r = 250$ nm, for which the values of the electric fields have been divided by respective maxima.

gain-assisted propagation of an SPP is involved in the discussions, such a configuration provides a suitable platform to include active media.⁵¹ More details about the criteria to choose an appropriate plasmonic waveguide are given in the Supporting Information. Moreover, the experimental bases to realize the proposed hybrid plasmonic waveguide are mature, and the very structure has been demonstrated in a series of photonic applications.^{7,51,59}

The material composition of the waveguide should be properly chosen according to specific operation wavelengths. We would set the wavelengths of the pump and down-converted photons at 0.775 and 1.55 μm , respectively. The substrate metal is better to be defined as silver due to its relatively low loss at the corresponding wavelength range.⁴⁷ As the gain compensation of the SPP is considered, the composition of the nanowire is chosen to be CdSe, which could be utilized as an active material at the pump wavelength range.^{51,60} The energy of the eigen-SPP mode supported in the hybrid structure mainly is concentrated in the gap,^{7,58} so the thin film between the substrate and nanowire should be formed by a suitable quadratic nonlinear optical material. A considerable choice is the organic polymer nonlinear material. On one hand, compared with ordinary nonlinear optical crystals, organic material is more available for complex geometry; on the other hand, the organic nonlinear material usually possesses an ultralarge quadratic nonlinear coefficient.⁴⁷ We actually consider a doped, cross-linked guest–host polymer, which has recently attracted a lively interest in nonlinear optics.^{47,61} Its effective second-order nonlinear coefficient reaches 619.4 pm/V,⁴⁷ which ensures a highly effective nonlinear interaction. Moreover, periodically poling technology of nonlinear optical polymer film is available for effective quasi-phase matching.^{62,63}

From Figure 3b, it is seen that there are two main geometric parameters of the structure, i.e., the thickness of organic film and the radius of the CdSe nanowire. Both of them have an important influence on the eigenmodes of the structure. In our simulations, they are set at 20 and 250 nm, respectively. The SPP modes are calculated through the finite element method (FEM). The effective indices of the pump and down-converted modes are equal to $1.72 + 0.0053i$ and $1.87 + 0.0031i$, respectively. The corresponding profiles of the dominant field component E_y are shown in Figure 3c and d. From the figures, it could be clearly seen that the majority of the energy of both the pump and down-converted field is concentrated in the region of the nonlinear organic film. The effective mode overlap is thus ultrahigh. The advantages of the considered configuration are presented. Besides the chosen structure, if the value of $\iint d\vec{r} \Phi_p(\vec{r}) \Phi_s^2(\vec{r})$ is the same but the overlap with the nonlinear organic film is different, we cannot achieve the same squeezing level. Moreover, as the intrinsic loss of the SPP mode is also an influencing factor, different loss corresponds to different squeezing results. Nevertheless, if there is a type of waveguide that can ensure that all these factors are identical, the same squeezing results can be acquired.

In the situation of ideal pump compensation, the nonlinear gain is calculated to be $(18.275A_p) \times 10^4 \text{ m}^{-1}$ based on eqs 4 and 12, where A_p is the amplitude of the pump field (the calculations are done based on normalized modes). The attenuation coefficient α_{PDC} is equal to $2.513 \times 10^4 \text{ m}^{-1}$, so the ratio $R_{\text{N/L}}$ should be $7.3A_p$. The degrees of squeezing and antisqueezing are calculated along the squeezing length according to different values of A_p based on eqs 12 and 13,

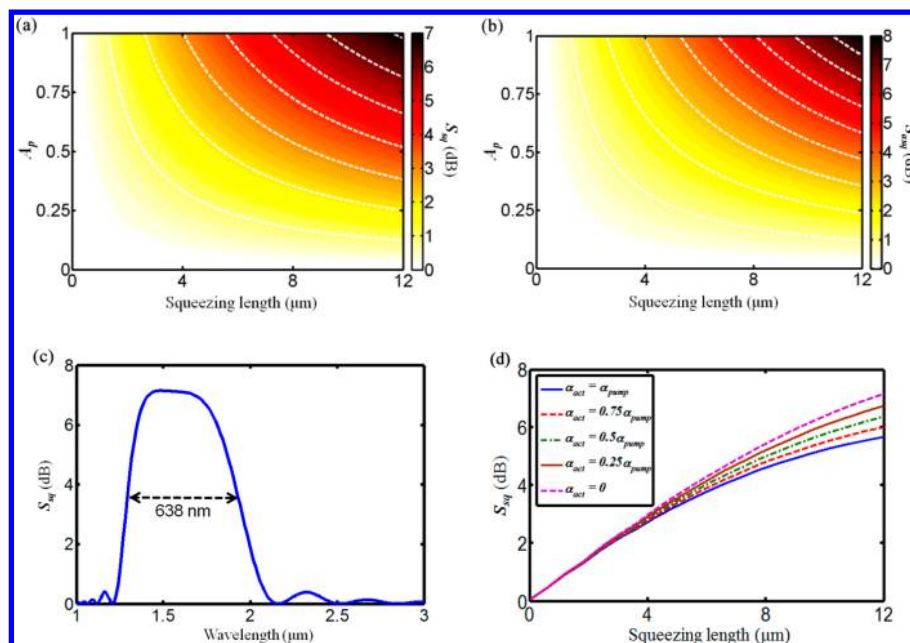


Figure 4. Squeezing results in the hybrid plasmonic waveguide system. The degrees of (a) squeezing and (b) antisqueezing vary with squeezing length according to different values of A_p . (c) Spectrum of squeezing with $L_{sq} = 12 \mu\text{m}$. The corresponding bandwidth is 638 nm. (d) Squeezing degree varies with squeezing length ($A_p = 1$) when the pump compensation is under 100%. The values of α_{act} correspond to different degrees of compensation.

which are shown in Figure 4a and b. In these two figure panels, the white dashed lines are the contours of squeezing and antisqueezing degrees. Due to intrinsic loss, the value of antisqueezing degree at a certain length is larger than that of squeezing degree with an equal A_p . However, choosing a proper device length could effectively suppress the antisqueezing noise. When the pump power is 1 W ($A_p = 1$), the squeezing degree reaches above 7 dB at a squeezing length of $\sim 12 \mu\text{m}$. For a single-path squeezing process, that is an ultrahigh value in a really short distance.

Such an advantage endows the squeezing system of SPP with great value for the integration of quantum circuits, which is essential for practical applications of quantum systems.^{64–66} On the contrary, in conventional squeezing systems based on nonlinear optical crystals, the squeezing efficiency is usually quite low in a single path even for a sample of several centimeters, so optical cavities are necessary for increasing the effective squeezing length.^{34–36} To ensure the squeezing result, the system becomes bulky. Another set of systems based on atomic vapor has been utilized for single-path squeezing,^{67,68} but the operations of a vapor bring challenges for integrated quantum applications. Moreover, owing to the short interaction length, the band of the squeezing spectrum is as wide as 481.7 THz (corresponding to 638 nm), as shown in Figure 4c. For the bulk crystal and atomic vapor systems, it is hard to obtain such a wide squeezing band while maintaining a large degree of squeezing. The calculated value of the bandwidth is more advantageous than that of the chirped quasi-phase-matching system which is known to possess a wide band squeezing spectrum.⁵⁶ In addition, the system is shown to have a good tolerance to attenuation. The degree of squeezing according to pump compensation under 100% is calculated and plotted against squeezing length in Figure 4d. It is seen that the squeezing is not seriously weakened even for the situation with no compensation ($\alpha_{act} = \alpha_{pump}$). The corresponding reduction

is about 1.4 dB. As the compensation increases (while α_{act} decreases), the quantity of reduction is lower.

CONCLUSIONS

The plasmonic system provides an attracting platform for quantum photonic applications, which brings a great deal of novel characteristics. Many passive plasmonic devices with various functions have been utilized in different quantum circuits, such as single SPP emitters,²² quantum coherence devices,^{24,25} and quantum plasmonic sensors.⁶⁹ Moreover, the nonlinear interactions of SPPs offer opportunities for active plasmonic quantum devices, which take the plasmonic system a step further for function-integrated quantum circuits. Besides the squeezed SPP state generator proposed in this paper, the entangled SPP state may also be available from the parametric down conversion process of SPPs. The intrinsic loss of the plasmonic mode makes the corresponding states quite different from photonic states generated in conventional optical setups, which may introduce new degrees of freedom into the plasmonic quantum systems.

In summary, we theoretically investigate the generation of a squeezed SPP state through parametric down conversion. The differential approach to derive the squeezing result is proposed, and analytic expressions for the special case in which down-converted frequencies are degenerate are obtained. The influence of intrinsic loss of the SPP is discussed in detail. Although the loss brings a squeezing limit, it could be improved to an acceptable degree through increasing nonlinear gain. Moreover, the dynamic process of squeezing is promoted by the loss, and the squeezing length corresponding to a certain squeezing degree is shortened. As an illustration, the squeezing result in a hybrid plasmonic waveguide structure is calculated. The squeezing degree of the generated squeezed SPP state could reach above 7 dB with a propagation length of only about $12 \mu\text{m}$ in a single path. Moreover, the squeezing bandwidth is calculated to be 481.7 THz. The tolerance of the system to loss

is also shown to be good. These characteristics make the device significant for constructing integrated quantum photonic circuits. In fact, there are still many interesting quantum properties of SPPs to be fully explored, which is a fast developing research area in quantum photonics.

METHODS

Deriving the Final Squeezing State in the Single-Mode Squeezing Case. When the pump SPP is 100% compensated, the transformation matrices of operators in all dz -cells are the same. Starting from the first dz -cell, the derivation process is as follows:

(i) Applying the local lossless Hamiltonian, the equation is expressed as

$$\begin{bmatrix} a_{z1,sq} \\ a_{z1,sq}^\dagger \end{bmatrix} = \begin{bmatrix} \cosh[(\Omega_{1,g} n_{PDC}/c) dz] & -\sinh[(\Omega_{1,g} n_{PDC}/c) dz] \\ -\sinh[(\Omega_{1,g} n_{PDC}/c) dz] & \cosh[(\Omega_{1,g} n_{PDC}/c) dz] \end{bmatrix} \begin{bmatrix} a_{in} \\ a_{in}^\dagger \end{bmatrix} \quad (17)$$

It is calculated to be

$$\begin{cases} a_{z1,sq} = \cosh[(\Omega_{1,g} n_{PDC}/c) dz] a_{in} \\ \quad - \sinh[(\Omega_{1,g} n_{PDC}/c) dz] a_{in}^\dagger \\ a_{z1,sq}^\dagger = -\sinh[(\Omega_{1,g} n_{PDC}/c) dz] a_{in} \\ \quad + \cosh[(\Omega_{1,g} n_{PDC}/c) dz] a_{in}^\dagger \end{cases} \quad (18)$$

$$\begin{aligned} & \begin{bmatrix} \cosh[(n+1)(\Omega_{1,g} n_{PDC}/c) dz] a_j - \sinh[(n+1)(\Omega_{1,g} n_{PDC}/c) dz] a_j^\dagger \\ -\sinh[(n+1)(\Omega_{1,g} n_{PDC}/c) dz] a_j + \cosh[(n+1)(\Omega_{1,g} n_{PDC}/c) dz] a_j^\dagger \end{bmatrix} \\ &= \begin{bmatrix} \cosh[(\Omega_{1,g} n_{PDC}/c) dz] & -\sinh[(\Omega_{1,g} n_{PDC}/c) dz] \\ -\sinh[(\Omega_{1,g} n_{PDC}/c) dz] & \cosh[(\Omega_{1,g} n_{PDC}/c) dz] \end{bmatrix} \begin{bmatrix} \cosh[n(\Omega_{1,g} n_{PDC}/c) dz] a_j - \sinh[n(\Omega_{1,g} n_{PDC}/c) dz] a_j^\dagger \\ -\sinh[n(\Omega_{1,g} n_{PDC}/c) dz] a_j + \cosh[n(\Omega_{1,g} n_{PDC}/c) dz] a_j^\dagger \end{bmatrix} \quad (21) \end{aligned}$$

In this expression, $\{a_j^\dagger, a_j\}$ could be $\{a_{in}^\dagger, a_{in}\}$ or $\{a_{z,v}^\dagger, a_{z,v}\}$. Through direct calculations, this equation is not hard to confirm. On the basis of these analyses, the final formation of the squeezed SPP state could be obtained as eq 9.

ASSOCIATED CONTENT

Supporting Information

The Supporting Information is available free of charge on the ACS Publications website at DOI: 10.1021/acsphtonic.6b00420.

The proof of the equivalence of the beam splitter model and the approach of the master equation; the criteria to select a suitable plasmonic waveguide for the exhibition of a squeezed SPP (PDF)

AUTHOR INFORMATION

Corresponding Authors

*E-mail: lijian.zhang@nju.edu.cn.

*E-mail: yqlu@nju.edu.cn.

Notes

The authors declare no competing financial interest.

ACKNOWLEDGMENTS

This work was supported by the National Natural Science Foundation of China under Grants 61225026, 61322503,

(ii) Mixing the vacuum state, the corresponding operators are expressed as

$$\begin{aligned} a_{z1,out} &= \sqrt{T_{dz}} a_{z1,sq} + \sqrt{R_{dz}} a_{z1,v} \\ a_{z1,out}^\dagger &= \sqrt{T_{dz}} a_{z1,sq}^\dagger + \sqrt{R_{dz}} a_{z1,v}^\dagger \end{aligned} \quad (19)$$

Similarly, in the second dz -cell, we have

$$\begin{cases} a_{z2,sq} = \sqrt{T_{dz}} \{ \cosh[2(\Omega_{1,g} n_{PDC}/c) dz] a_{in} \\ \quad - \sinh[2(\Omega_{1,g} n_{PDC}/c) dz] a_{in}^\dagger \} \\ \quad + \sqrt{R_{dz}} \{ \cosh[(\Omega_{1,g} n_{PDC}/c) dz] a_{z1,v} \\ \quad - \sinh[(\Omega_{1,g} n_{PDC}/c) dz] a_{z1,v}^\dagger \} \\ a_{z2,sq}^\dagger = \sqrt{T_{dz}} \{ -\sinh[2(\Omega_{1,g} n_{PDC}/c) dz] a_{in} \\ \quad + \cosh[2(\Omega_{1,g} n_{PDC}/c) dz] a_{in}^\dagger \} \\ \quad + \sqrt{R_{dz}} \{ -\sinh[(\Omega_{1,g} n_{PDC}/c) dz] a_{z1,v} \\ \quad + \cosh[(\Omega_{1,g} n_{PDC}/c) dz] a_{z1,v}^\dagger \} \end{cases} \quad (20)$$

It is seen that the initial input state $\{a_{in}^\dagger, a_{in}\}$ is going on to be squeezed in this cell. Moreover, the squeezing of the vacuum state $\{a_{z1,v}^\dagger, a_{z1,v}\}$ also begins here. It indicates that in the plasmonic system a vacuum state is injected in at each z -position (for the initial input state, it could be treated as a vacuum state injected at $z = 0$) and squeezed in the remaining interaction region until the output port. To prove this deduction, according to the mathematical induction, it is necessary to show that

61490714, and 11474159, by the Fostering Program for NSFC under Contract No. 021314380040, and by the Program for Changjiang Scholars and Innovative Research Team at the University under Contract No. IRT13021. We thank the helpful discussions with Dr. Long Li in preparing the revised manuscript.

REFERENCES

- (1) Maier, S. A. *Plasmonics: Fundamentals and Applications*; Springer: New York, 2007.
- (2) Barnes, W. L.; Dereux, A.; Ebbesen, T. W. Surface plasmon subwavelength optics. *Nature* **2003**, *424*, 824–830.
- (3) Gramotnev, D. K.; Bozhevolnyi, S. I. Plasmonics beyond the diffraction limit. *Nat. Photonics* **2010**, *4*, 83–91.
- (4) Lal, S.; Link, S.; Halas, N. J. Nano-optics from sensing to waveguiding. *Nat. Photonics* **2007**, *1*, 641–648.
- (5) Berini, P.; De Leon, I. Surface plasmon-polariton amplifiers and lasers. *Nat. Photonics* **2012**, *6*, 16–24.
- (6) Bozhevolnyi, S. I.; Volkov, V. S.; Devaux, E.; Laluet, J. Y.; Ebbesen, T. W. Channel plasmon subwavelength waveguide components including interferometers and ring resonators. *Nature* **2006**, *440*, 508–511.
- (7) Oulton, R. F.; Sorger, V. J.; Zentgraf, T.; Ma, R. M.; Gladden, C.; Dai, L.; Bartal, G.; Zhang, X. Plasmon lasers at deep subwavelength scale. *Nature* **2009**, *461*, 629–632.
- (8) Zhang, W. H.; Martin, O. J. F. A universal law for plasmon resonance shift in biosensing. *ACS Photonics* **2015**, *2*, 144–150.

- (9) Nikolajsen, T.; Leosson, K.; Bozhevolnyi, S. I. Surface plasmon polariton based modulators and switches operating at telecom wavelengths. *Appl. Phys. Lett.* **2004**, *85*, 5833–5835.
- (10) Dittlbacher, H.; Krenn, J. R.; Schider, G.; Leitner, A.; Aussenegg, F. R. Two-dimensional optics with surface plasmon polaritons. *Appl. Phys. Lett.* **2002**, *81*, 1762–1764.
- (11) Feng, J.; Siu, V. S.; Roelke, A.; Mehta, V.; Rhieu, S. Y.; Tayhas, G.; Palmore, R.; Pacifici, D. Nanoscale plasmonic interferometers for multispectral, high-throughput biochemical sensing. *Nano Lett.* **2012**, *12*, 602–609.
- (12) Ming, Y.; Wu, Z. J.; Wu, H.; Xu, F.; Lu, Y. Q. Surface plasmon interferometer based on wedge metal waveguide and its sensing applications. *IEEE Photonics J.* **2012**, *4*, 291–299.
- (13) Tame, M. S.; McEnery, K. R.; Özdemir, S. K.; Lee, J.; Maier, S. A.; Kim, M. S. Quantum plasmonics. *Nat. Phys.* **2013**, *9*, 329–340.
- (14) Jacob, Z. Quantum plasmonics. *MRS Bull.* **2012**, *37*, 761–767.
- (15) Altevischer, E.; van Exter, M. P.; Woerdman, J. P. Plasmon-assisted transmission of entangled photons. *Nature* **2002**, *418*, 304–306.
- (16) Fasel, S.; Robin, F.; Moreno, E.; Erni, D.; Gisin, N.; Zbinden, H. Energy-time entanglement preservation in plasmon-assisted light transmission. *Phys. Rev. Lett.* **2005**, *94*, 110501.
- (17) Fasel, S.; Halder, M.; Gisin, N.; Zbinden, H. Quantum superposition and entanglement of mesoscopic plasmons. *New J. Phys.* **2006**, *8*, 13.
- (18) Ren, X. F.; Guo, G. P.; Huang, Y. F.; Li, C. F.; Guo, G. C. Plasmon-assisted transmission of high-dimensional orbital angular momentum entangled state. *Europhys. Lett.* **2006**, *76*, 753–759.
- (19) Tame, M. S.; Lee, C.; Lee, J.; Ballester, D.; Paternostro, M.; Zayats, A. V.; Kim, M. S. Single-photon excitation of surface plasmon polaritons. *Phys. Rev. Lett.* **2008**, *101*, 190504.
- (20) Ballester, D.; Tame, M. S.; Lee, C.; Lee, J.; Kim, M. S. Long-range surface-plasmon-polariton excitation at the quantum level. *Phys. Rev. A: At, Mol., Opt. Phys.* **2009**, *79*, 053845.
- (21) Di Martino, G.; et al. Quantum statistics of surface plasmon polaritons in metallic stripe waveguides. *Nano Lett.* **2012**, *12*, 2504–2508.
- (22) Akimov, A. V.; Mukherjee, A.; Yu, C. L.; Chang, D. E.; Zibrov, A. S.; Hemmer, P. R.; Park, H.; Lukin, M. D. Generation of single optical plasmons in metallic nanowires coupled to quantum dots. *Nature* **2007**, *450*, 402–406.
- (23) Kolesov, R.; Grotz, B.; Balasubramanian, G.; Stöhr, R. J.; Nicolet, A. A. L.; Hemmer, P. R.; Jelezko, F.; Wrachtrup, J. Wave-particle duality of single surface plasmon polaritons. *Nat. Phys.* **2009**, *5*, 470–474.
- (24) Di Martino, G.; Sonnefraud, Y.; Tame, M. S.; Kéna-Cohen, S.; Dieleman, F.; Özdemir, S. K.; Kim, M. S.; Maier, S. A. Observation of quantum interference in the plasmonic Hong-Ou-Mandel effect. *Phys. Rev. Appl.* **2014**, *1*, 034004.
- (25) Fakonas, J. S.; Lee, H.; Kelaita, Y. A.; Atwater, H. A. Two-plasmon quantum interference. *Nat. Photonics* **2014**, *8*, 317–320.
- (26) McKenzie, K.; Shaddock, D. A.; McClelland, D. E.; Buchler, B. C.; Lam, P. K. Experimental demonstration of a squeezing-enhanced power-recycled Michelson interferometer for gravitational wave detection. *Phys. Rev. Lett.* **2002**, *88*, 231102.
- (27) Zhang, L. J.; Xiao, M. Towards quantum-enhanced precision measurements: Promise and challenges. *Chin. Phys. B* **2013**, *22*, 110310.
- (28) Braunstein, S. L.; Van Loock, P. Quantum information with continuous variables. *Rev. Mod. Phys.* **2005**, *77*, 513–577.
- (29) Martín-Cano, D.; Haakh, H. R.; Murr, K.; Agio, M. Large suppression of quantum fluctuations of light from a single emitter by an optical nanostructure. *Phys. Rev. Lett.* **2014**, *113*, 263605.
- (30) Huck, A.; Smolka, S.; Lodahl, P.; Sørensen, A. S.; Boltasseva, A.; Janousek, J.; Andersen, U. L. Demonstration of quadrature-squeezed surface plasmons in a gold waveguide. *Phys. Rev. Lett.* **2009**, *102*, 246802.
- (31) Miyazaki, H. T.; Kurokawa, Y. Squeezing visible light waves into a 3-nm-thick and 55-nm-long plasmon cavity. *Phys. Rev. Lett.* **2006**, *96*, 097401.
- (32) Wang, D.; Xia, C. Q.; Wang, Q.; Wu, Y.; Liu, F.; Zhang, Y.; Xiao, M. Feedback-optimized extraordinary optical transmission of continuous-variable entangled states. *Phys. Rev. B: Condens. Matter Mater. Phys.* **2015**, *91*, 121406.
- (33) Scully, M. O.; Zubairy, M. S. *Quantum Optics*; Cambridge University Press, 1997.
- (34) Wu, L. A.; Kimble, H. J.; Hall, J. L.; Wu, H. F. Generation of squeezed states by parametric down conversion. *Phys. Rev. Lett.* **1986**, *57*, 2520–2523.
- (35) Wu, L. A.; Xiao, M.; Kimble, H. J. Squeezed states of light from an optical parametric oscillator. *J. Opt. Soc. Am. B* **1987**, *4*, 1465–1475.
- (36) Pereira, S. F.; Xiao, M.; Kimble, H. J.; Hall, J. L. Generation of squeezed light by intracavity frequency doubling. *Phys. Rev. A: At, Mol., Opt. Phys.* **1988**, *38*, 4931–4934.
- (37) Slusher, R. E.; Hollberg, L. W.; Yurke, B.; Mertz, J. C.; Valley, J. F. Observation of Squeezed States Generated by Four-Wave Mixing in an Optical Cavity. *Phys. Rev. Lett.* **1985**, *55*, 2409–2412.
- (38) Kwiat, P. G.; Mattle, K.; Weinfurter, H.; Zeilinger, A.; Sergienko, A. V.; Shih, Y. H. New high-intensity source of polarization-entangled photon pairs. *Phys. Rev. Lett.* **1995**, *75*, 4337–4341.
- (39) Li, X. Y.; Voss, P. L.; Sharping, J. E.; Kumar, P. Optical-fiber source of polarization-entangled photons in the 1550 nm telecom band. *Phys. Rev. Lett.* **2005**, *94*, 053601.
- (40) Pan, J. W.; Chen, Z. B.; Lu, C. Y.; Weinfurter, H.; Zeilinger, A.; Zukowski, M. Multi-photon entanglement and interferometry. *Rev. Mod. Phys.* **2012**, *84*, 777–838.
- (41) Ou, Z. Y. *J. Multi-photon Quantum Interference*; Springer: New York, 2007.
- (42) Kauranen, M.; Zayats, A. V. Nonlinear plasmonics. *Nat. Photonics* **2012**, *6*, 737–748.
- (43) Wu, Z. J.; Hu, X. K.; Yu, Z. Y.; Hu, W.; Xu, F.; Lu, Y. Q. Nonlinear plasmonic frequency conversion through quasiphase matching. *Phys. Rev. B: Condens. Matter Mater. Phys.* **2010**, *82*, 155107.
- (44) Lu, F. F.; Li, T.; Xu, J.; Xie, Z. D.; Li, L.; Zhu, S. N.; Zhu, Y. Y. Surface plasmon polariton enhanced by optical parametric amplification in nonlinear hybrid waveguide. *Opt. Express* **2011**, *19*, 2858–2865.
- (45) Lu, F. F.; Li, T.; Hu, X. P.; Cheng, Q. Q.; Zhu, S. N.; Zhu, Y. Y. Efficient second-harmonic generation in nonlinear plasmonic waveguide. *Opt. Lett.* **2011**, *36*, 3371–3373.
- (46) Davoyan, A. R.; Shadrivov, I. V.; Kivshar, Y. S. Quadratic phase matching in nonlinear plasmonic nanoscale waveguides. *Opt. Express* **2009**, *17*, 20063–20068.
- (47) Zhang, J. H.; Cassan, E.; Gao, D. S.; Zhang, X. L. Highly efficient phase-matched second harmonic generation using an asymmetric plasmonic slot waveguide. *Opt. Express* **2013**, *21*, 14876–14887.
- (48) Pigozzo, F. M.; Modotto, D.; Wabnitz, S. Second harmonic generation by modal phase matching involving optical and plasmonic modes. *Opt. Lett.* **2012**, *37*, 2244–2246.
- (49) This assumption is valid within a limited propagation length. When the energy of the pump field is reduced to the quantum level, it can no longer be treated classically. However, approaches such as gain compensation and hybrid structure are effective to extend the propagation length. Moreover, we are going to show that there is an effective length for the squeezing of an SPP in the following text. Inside this length, this assumption is ensured to be valid.
- (50) Ming, Y.; Wu, Z. J.; Tan, A. H.; Hu, X. K.; Xu, F.; Lu, Y. Q. Quantum entanglement based on surface phonon polaritons in condensed matter systems. *AIP Adv.* **2013**, *3*, 042122.
- (51) Liu, N.; Wei, H.; Li, J.; Wang, Z.; Tian, X.; Pan, A.; Xu, H. X. Plasmonic amplification with ultra-high optical gain at room temperature. *Sci. Rep.* **2013**, *3*, 1967.
- (52) Caves, C. M.; Crouch, D. D. Quantum wideband traveling-wave analysis of a degenerate parametric amplifier. *J. Opt. Soc. Am. B* **1987**, *4*, 1535–1545.

(53) Jeffers, J. R.; Imoto, N.; Loudon, R. Quantum optics of traveling-wave attenuators and amplifiers. *Phys. Rev. A: At., Mol., Opt. Phys.* **1993**, *47*, 3346–3359.

(54) Antonosyan, D. A.; Solntsev, A. S.; Sukhorukov, A. A. Effect of loss on photon-pair generation in nonlinear waveguide arrays. *Phys. Rev. A: At., Mol., Opt. Phys.* **2014**, *90*, 043845.

(55) Leonhardt, U. Quantum statistics of a lossless beam splitter: SU(2) symmetry in phase space. *Phys. Rev. A: At., Mol., Opt. Phys.* **1993**, *48*, 3265–3277.

(56) Horoshko, D. B.; Kolobov, M. I. Towards single-cycle squeezing in chirped quasi-phase-matched optical parametric down-conversion. *Phys. Rev. A: At., Mol., Opt. Phys.* **2013**, *88*, 033806.

(57) Caves, C. M.; Crouch, D. D. Quantum wideband traveling-wave analysis of a degenerate parametric amplifier. *J. Opt. Soc. Am. B* **1987**, *4*, 1535–1545.

(58) Oulton, R. F.; Sorger, V. J.; Genov, D. A.; Pile, D. F. P.; Zhang, X. A hybrid plasmonic waveguide for subwavelength confinement and long-range propagation. *Nat. Photonics* **2008**, *2*, 496–500.

(59) Sidiropoulos, T. P. H.; Röder, R.; Geburt, S.; Hess, O.; Maier, S. A.; Ronning, C.; Oulton, R. F. Ultrafast plasmonic nanowire lasers near the surface plasmon frequency. *Nat. Phys.* **2014**, *10*, 870–876.

(60) Wang, G. Z.; Jiang, X. S.; Zhao, M.; Ma, Y.; Fan, H.; Yang, Q.; Tong, L. M.; Xiao, M. Microlaser based on a hybrid structure of a semiconductor nanowire and a silica microdisk cavity. *Opt. Express* **2012**, *20*, 29472–29478.

(61) Enami, Y.; Enami, Y.; Derose, C. T.; Mathine, D.; Loychik, C.; Greenlee, C.; Norwood, R. A.; Kim, T. D.; Luo, J.; Tian, Y.; Jen, A. K. Y.; Peyghambarian, N. Hybrid polymer/sol-gel waveguide modulators with exceptionally large electro-optic coefficients. *Nat. Photonics* **2007**, *1*, 180–185.

(62) Michelotti, F.; Toussaere, E. Pulse poling of side-chain and crosslinkable copolymers. *J. Appl. Phys.* **1997**, *82*, 5728–5744.

(63) Herr, R. P.; Schadt, M.; Schmitt, K. Optically Non-linear Polymeric Coatings. US Patent No. 5447662, 1995.

(64) Crespi, A.; Ramponi, R.; Osellame, R.; Sansoni, L.; Bongioanni, I.; Sciarino, F.; Vallone, G.; Mataloni, P. Integrated photonic quantum gates for polarization qubits. *Nat. Commun.* **2011**, *2*, 566.

(65) Ming, Y.; Tan, A. H.; Wu, Z. J.; Chen, Z. X.; Xu, F.; Lu, Y. Q. Tailoring entanglement through domain engineering in a lithium niobate waveguide. *Sci. Rep.* **2014**, *4*, 4812.

(66) Ming, Y.; Wu, Z. J.; Cui, G. X.; Tan, A. H.; Xu, F.; Lu, Y. Q. Integrated source of tunable nonmaximally mode-entangled photons in a domain-engineered lithium niobate waveguide. *Appl. Phys. Lett.* **2014**, *104*, 171110.

(67) Corzo, N. V.; Glorieux, Q.; Marino, A. M.; Clark, J. B.; Glasser, R. T.; Lett, P. D. Rotation of the noise ellipse for squeezed vacuum light generated via four-wave mixing. *Phys. Rev. A: At., Mol., Opt. Phys.* **2013**, *88*, 043836.

(68) Mikhailov, E. E.; Novikova, I. Low-frequency vacuum squeezing via polarization self-rotation in Rb vapor. *Opt. Lett.* **2008**, *33*, 1213–1215.

(69) Lee, C.; Dieleman, F.; Lee, J.; Rockstuhl, C.; Maier, S. A.; Tame, M. Quantum plasmonic sensing: Beyond the shot-noise and diffraction limit. *ACS Photonics* **2016**, *3*, 992–999.